J|A|C|S
COMMUNICATIONS

Superresolution Imaging of Targeted Proteins in Fixed and Living Cells Using Photoactivatable Organic Fluorophores

Hsiao-lu D. Lee,[†] Samuel J. Lord,[†] Shigeki Iwanaga,[†] Ke Zhan,[‡] Hexin Xie,[‡] Jarrod C. Williams,[||]
Hui Wang,[||] Grant R. Bowman,[§] Erin D. Goley,[§] Lucy Shapiro,[§] Robert J. Twieg,[||] Jianghong Rao,[‡]
and W. E. Moerner*,[†]

*Departments of Chemistry, Radiology, Developmental Biology, Stanford University, Stanford, California 94305, and
Department of Chemistry, Kent State University, Kent, Ohio 44244*

Received May 21, 2010; E-mail: wmoerner@stanford.edu

Abstract: Superresolution imaging techniques based on sequential imaging of sparse subsets of single molecules require fluorophores whose emission can be photoactivated or photoswitched. Because typical organic fluorophores can emit significantly more photons than average fluorescent proteins, organic fluorophores have a potential advantage in super-resolution imaging schemes, but targeting to specific cellular proteins must be provided. We report the design and application of HaloTag-based target-specific azido DCDHFs, a class of photoactivatable push−pull fluorogens which produce bright fluorescent labels suitable for single-molecule superresolution imaging in live bacterial and fixed mammalian cells.

Recently, sequential imaging of sparse subsets of photoactivatable/photoswitchable single-molecule fluorophores has enabled optical imaging beyond the diffraction limit (DL), providing insight into the subdiffraction world (e.g., PALM, FPALM, STORM).[1−3] These single-molecule superresolution (SR) techniques have provided the impetus for development of new controllable fluorophores with large numbers of emitted photons N, because the achievable resolution[4] scales as $1/\sqrt{N}$. Most previous SR experiments in living cells[5] have used photocontrollable fluorescent proteins.[6−9] However, despite having the advantage of being target-specific, fluorescent proteins on average provide 10-fold fewer photons before photobleaching than good organic fluorophores.[10,11] Small organic fluorophores have the additional benefit of synthetic design flexibility for tuning target specificity, spectral wavelength, solubility, and other desired properties. Therefore, targeted bright organic fluorophores which are compatible with the live-cell environment and which can be turned on and/or off would be advantageous. While targeted fluorogens which activate via esterase-mediated cleavage have been previously demonstrated,[12] optical control of the emitting concentration is necessary for SR.[13]

Many biological processes can be interrupted by fixing (i.e., killing) cells, which is required for the immunostaining used in most SR experiments that rely on organic fluorophores.[16,17] While fixation can be useful, there is a need for techniques and probes that can be used for SR imaging in *living* cells. Single-molecule imaging in living cells using exogenous fluorophores faces the dual hurdles of cell permeability and targeted labeling.[5] There are exceptions in the literature that did not use fixation and immunostaining. For instance, Heilemann et al.[17] imaged mRNA in living cells using oligomers labeled with

Scheme 1. Photochemical Activation Produces **2** from **1**[a]
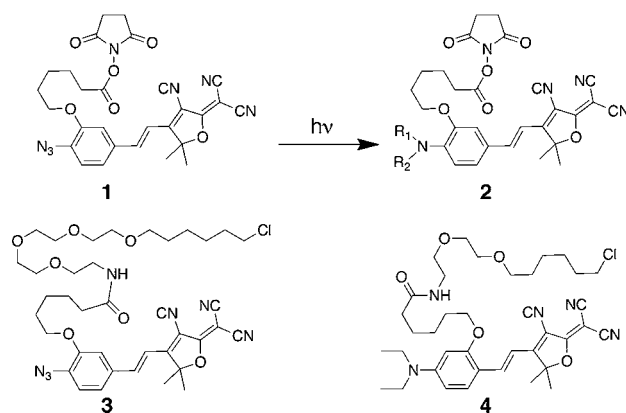
[a] A mixture of photoproducts is produced,[14,15] but the primary amine with $R_1=R_2=H$ is the significant product (see Table 1 for reaction yield of primary amine). HaloTag versions of **1** and a separate fluorophore are also shown (**3** and **4**).

small organic fluorophores and Conley et al.[18] labeled the external lysines of bacterial cells using a Cy3-Cy5 heterodimer. Very recently, fluorophores were targeted with trimethoprim and intrinsic cellular reductants enabled photoinduced blinking.[19] These examples demonstrated some possibilities for live-cell labeling and SR, but there is still a need for photoactivatable organic labels for SR imaging because each molecule is localized only once, while, with blinking or photoswitching, each molecule can be localized a variable number of times.

Here we present a target-specific photoactivatable organic fluorophore for use inside living and fixed cells, **3**, based on the commercial HaloTag targeting approach.[20−22] This method requires a genetic fusion to the HaloEnzyme (HaloEnz), which forms a covalent linkage to the HaloTag substrate, thus labeling the protein of interest (i.e., a protein-HaloEnz-HaloTag-fluorophore covalent unit). Specifically, we present the following: (i) the basic photophysical properties of a new targeted photoactivatable probe; (ii) proof-of-principle labeling of known structures in fixed and living mammalian cells validated by costaining with antibodies or cotransfection with fluorescent proteins; (iii) specific SR imaging of microtubules in a mammalian cell with quantification of resolution enhancement; (iv) demonstration of targeted labeling in living bacteria with diffraction-limited imaging; and finally, (v) SR imaging of poorly understood structures inside living bacteria.

As molecules with bright emission for single-molecule imaging, dicyanomethylenedihydrofuran (DCDHF) push−pull fluorophores emit millions of photons before photobleaching and can enter living cells.[15,23] Recently, we reported a photoactivatable DCDHF fluorogen

[†] Department of Chemistry, Stanford University.
[‡] Department of Radiology, Stanford University.
[§] Department of Developmental Biology, Stanford University.
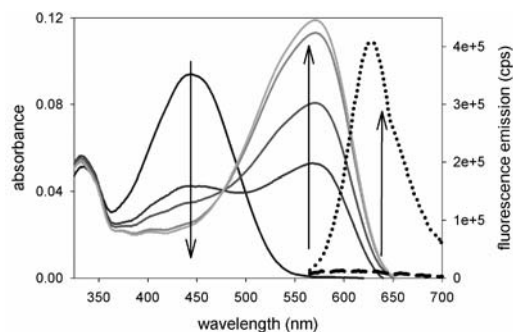[||] Department of Chemistry, Kent State University.

Figure 1. Absorption of **1** in ethanol decreases during irradiation with 1.1 mW/cm^2 at 385 nm shown at 15, 30, 90, and 150 s (left down arrow). Concurrently, the absorption of amine photoproduct **2** grows proportionally (center up arrow). The bright fluorescence from **2** when pumped at 550 nm is the dotted curve; the heavy dashed curve is dim fluorescence from the original sample of **1** (the small emission signal is most likely from the preactivated amine contaminants in the azide sample). Preactivation can be minimized by keeping the samples in complete darkness. Compound **3** has the same photophysical properties as **1**.

based on photocaging the fluorescence by replacing the amine donor with a poorly donating but photolabile azide, which can then be converted back to an amine using low-intensity blue light.[14] Azido DCDHF fluorogens exhibit high turn-on ratios (the increase in emission from the fluorescent form compared to the dark fluorogen) of 325−1270-fold, an attractive property for SR imaging.[15] (For a detailed discussion of the photophysical properties of the fluorogens, as well as the methods used to characterize them, see refs 11 and 15.)

Table 1. Photophysical/Photochemical Parameters

	$\lambda_{abs,azide}$ (nm)[b]	$\lambda_{abs,amine}/\lambda_{fl,amine}$ (nm)[c]	Yield[d]	Φ_P[e]
DCDHF-V-P-azide[a]	424	570/613	65%	0.0059
1 (and **3**)	443	572/627	∼50%	0.095
4	−	598/629	−	−

[a] DCDHF-V-P-azide is the earlier underivatized azido-DCDHF from ref 9 for comparison. [b] Peak absorbance for azido fluorogen. [c] Absorbance and fluorescence peak wavelengths of the amino fluorophore. [d] Overall chemical reaction yield to the primary fluorescent amine. [e] Photoconversion quantum yield of azido fluorogens to any product (i.e., the probability of photoconverting after absorbing one photon). For reference, the value of Φ_P for mEos is on the order of 10^{-5} (see ref 11 for more detailed comparisons). For all DCDHFs, the fluorescence quantum yield of the photoactivated form varies greatly depending on the precise nanoenvironment, typically <0.1% in buffer to >30% when rigidized (e.g., in the membrane or when bound to proteins).[23] For measurement details, see SI. Compound **3** has the same photophysical properties as **1**.

Compared with the original DCDHF-V-P-azide,[14] **3** exhibits similar spectral changes upon optical pumping of the aryl azide (Figure 1) but a higher photoconversion quantum yield (Φ_P, see Table 1). Presumably the oxygen on the aryl azide stabilizes the intermediate nitrene, making photoconversion more favorable.[14,15,24] The photoconversion of **3** was so sensitive such that an additional activating blue laser was not necessary; instead, the diffuse ambient light (e.g., the blue light emitted from a nearby computer monitor in an otherwise dark room) was sufficient to activate sparse sets of the fluorogen. The thermal activation rate and activation by the 594 nm imaging laser were significantly lower, as measured in complete darkness in a covered sample (see Supporting Information (SI)). Because the fluorogen's sensitivity to photoconversion is so high, it was possible to set the level of the ambient light such that the bleaching rate from 594 nm pumping was similar to the activation rate. For instance, with room lights off and a nearby computer monitor on, we maintained a steady-state concentration of isolated emitters. This reduced the

complexity of the experiment by allowing the use of only one laser.[17] Moreover, because no blue or UV laser was necessary for activation, photodamage to the imaging sample was greatly reduced. (The drawback to this high sensitivity is that it increases the difficulty of preventing photoactivation before imaging. We successfully minimized preactivation by performing all preparations in complete darkness or under dim red lights only.)

We verified the specificity of **3** in mammalian culture. Wild-type HeLa cells and HeLa cells transfected to express HaloEnz-α-tubulin were stained live with **3**, fixed, and immunostained with Alexa488-mAb to α-tubulin. Fluorescence images after photoactivation clearly demonstrate that **3** is only retained in the cells that expressed-HaloEnz-α-tubulin (Figure 2A−G). Next, live CHO cells were cotransfected with HaloEnz-α-tubulin and α-tubulin-eGFP, and the labeling by **3** was shown to colocalize well with the eGFP labeling (Figure 2H−I).
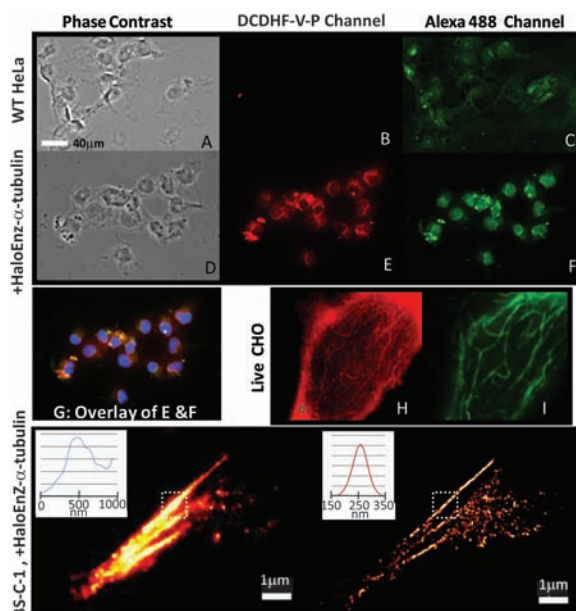

Figure 2. Evidence that the HaloTag-targeted fluorogen correctly labels specific proteins and enables SR imaging in mammalian cells. (A) Phase image of fixed WT HeLa cells. (B) The cells in A imaged in the DCDHF-V-P channel. (C) The cells in A imaged in the Alexa488 channel. (D) Phase image of fixed HeLa expressing HaloEnz-α-tubulin labeled with **3**. (E) The cells in D imaged in the DCDHF-V-P channel. (F) The cells in D imaged in Alexa488 channel. (G) Overlay of E, F, and additional blue DAPI channel to show nuclei. (H) Live CHO cells cotransfected to express both HaloEnz-α-tubulin and α-tubulin-eGFP labeled with **3** and imaged in DCDHF-V-P channel. (I) Cells from H imaged in the EGFP channel. (The higher background in H may be the result of nonspecific binding and imperfect washing of untargeted fluorophores.) (J) Fixed BS-C-1 cells expressing HaloEnz-α-tubulin labeled with **3** imaged using conventional diffraction-limited imaging. Indicated microtubule measures 450 ± 40 nm fwhm. (K) Same cell as J with SR imaging. Indicated microtubule measures 85 ± 15 nm fwhm. See SI for sample preparation procedures.

Most importantly, BS-C-1 cells were transfected with HaloEnz-α-tubulin, fixed, stained with **3**, and washed before SR imaging by PALM. Comparing DL and SR fluorescence images (Figure 2J,K), the microtubule structure is clearly imaged with a resolution beyond the optical diffraction limit. After corroborating the utility of the DCDHF fluorophores for labeling known structures in mammalian cells, we then moved our attention to cells with protein organization that is not fully understood.

Bacteria are tiny (about a thousand bacteria could fit within the volume of one HeLa cell), and the details of protein localization in prokaryotes are poorly understood, yet essential for function and phenotype.[25] DL imaging of labeled proteins in bacteria only

produces diffuse blobs, complicating meaningful interpretation. For these reasons, living bacterial studies benefit greatly from SR imaging.[11,26] We used HaloTag-DCDHFs to highlight protein localization patterns in live *Caulobacter crescentus* bacteria,[26−29] an organism which features the biologically interesting ability to divide asymmetrically. Elucidating the mechanisms of asymmetric cell division and intracellular organization requires understanding how cytoskeletal proteins localize through the life cycle of the cell.[25] In this Communication, a polar protein PopZ[27] and midplane proteins FtsZ[28] and AmiC[29] were expressed as HaloEnz fusions. PopZ, FtsZ, and AmiC have distinct roles: PopZ anchors the chromosomal origin at the "swarmer" pole; FtsZ and AmiC are recruited to the midplane and are components of the cell division machinery.[25] DL imaging using HaloTag targeting of the (nonphoto-activatable) fluorophore **4** shows correct PopZ localization at cell poles and FtsZ at the cellular division plane as expected (Figure 3), confirming that this HaloTag labeling system does not significantly interfere in phenotype.
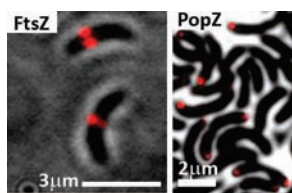

Figure 3. Diffraction-limited imaging of **4** inside live *C. crescentus* cells expressing fusion proteins to FtsZ and PopZ. These proteins localize as expected,[25] indicating that the HaloTag-DCDHF labeling does not disrupt typical cellular behavior.

SR images produced by photoactivation of fluorogen **3** not only display the expected localization patterns but also reveal additional detail unseen in the DL images of Figure 3. For PopZ at the cell pole, the protein forms an asymmetric cap-like structure with a curvature that hugs the shape of the bacterial membrane (Figure 4A−C). Also, in the case of AmiC, the protein localizes to the cellular midplane, as expected (Figure 4D−E). The SR images of AmiC may reveal a tighter organization than seen in DL microscopy, but further study is necessary
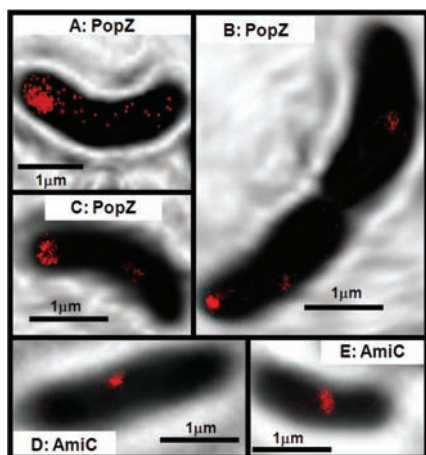

Figure 4. SR imaging of protein fusions inside live *C. crescentus* cells using **3**. (A−C) PopZ forms a polymeric network at the poles of the cells. Compared to the DL images in Figure 3, these SR images reveal distinct *shapes* of the PopZ structure, including the cap-like network in C. (D−E) AmiC is recruited to the division plane early in the cell cycle. These SR images indicate that AmiC may form a structure that hugs the membrane. For details of imaging and image processing, see SI. The SR images are extracted from localizations over 75 s with a mean localization precision of 32 ± 12 nm.

before any definitive statement can be made. In either case, these SR images provide new detail not available in DL images.

The target-specific DCDHF single-molecule fluorogen presented here represents the first successful installation of target specificity to small organic photoactivatable fluorogens for single-molecule SR imaging. Compared to existing schemes, the photoactivation of the fluorogen requires neither other additives (e.g., thiols for Cy5[30] or redox chemicals[17]) nor activation by UV light and thus can be used inside living cells. SR imaging has been directly demonstrated for fixed mammalian and live bacterial cells; additional effort to improve washout for live mammalian cells is an important topic for future work. This and future photoactivatable fluorogens should be helpful tools for SR imaging in the complex environment within the living cell.

Supporting Information Available: Procedures, chemical synthesis, analysis, additional figures, and complete ref 20. This material is available free of charge via the Internet at http://pubs.acs.org.

References

(1) Betzig, E.; Patterson, G. H.; Sougrat, R.; Lindwasser, O. W.; Olenych, S.; Bonifacino, J. S.; Davidson, M. W.; Lippincott-Schwartz, J.; Hess, H. F. *Science* **2006**, *313*, 1642–1645.
(2) Hess, S. T.; Girirajan, T. P. K.; Mason, M. D. *Biophys. J.* **2006**, *91*, 4258–4272.
(3) Rust, M. J.; Bates, M.; Zhuang, X. *Nat. Methods* **2006**, *3*, 793–795.
(4) Thompson, R. E.; Larson, D. R.; Webb, W. W. *Biophys. J.* **2002**, *82*, 2775–2783.
(5) Lord, S. J.; Lee, H. D.; Moerner, W. E. *Anal. Chem.* **2010**, *82* (6), 2192–2203.
(6) Dickson, R. M.; Norris, D. J.; Tzeng, Y. L.; Moerner, W. E. *Science* **1996**, *274*, 966–969.
(7) Ando, R.; Mizuno, H.; Miyawaki, A. *Science* **2004**, *306*, 1370–1373.
(8) Patterson, G. H.; Lippincott-Schwartz, J. *Science* **2002**, *297*, 1873–1877.
(9) Hess, S. T.; Gould, T. J.; Gudheti, M. V.; Maas, S. A.; Mills, K. D.; Zimmerberg, J. *Proc. Natl. Acad. Sci. U.S.A.* **2007**, *104*, 17370–17375.
(10) Schmidt, T.; Kubitscheck, U.; Rohler, D.; Nienhaus, U. *Single Mol.* **2002**, *3*, 327.
(11) Thompson, M. A.; Biteen, J. S.; Lord, S. J.; Conley, N. R.; Moerner, W. E. *Methods Enzym.* **2010**, *475*, 27–59.
(12) Watkins, R. W.; Lavis, L. D.; Kung, V. M.; Los, G. V.; Raines, R. T. *Org. Biomol. Chem.* **2009**, *7*, 3969–3975.
(13) Maurel, D.; Banala, S.; Laroche, T.; Johnsson, K. *ACS Chem. Biol.* **2010**, *5*, 507–516.
(14) Lord, S. J.; Conley, N. R.; Lee, H. D.; Samuel, R.; Liu, N.; Twieg, R. J.; Moerner, W. E. *J. Am. Chem. Soc.* **2008**, *130*, 9204–9205.
(15) Lord, S. J.; Lee, H. L.; Samuel, R.; Weber, R.; Liu, N.; Conley, N. R.; Thompson, M. A.; Twieg, R. J.; Moerner, W. E. *J. Phys. Chem. B* **2009**, ASAP (http://dx.doi.org/10.1021/jp907080r).
(16) Folling, J.; Bossi, M.; Bock, H.; Medda, R.; Wurm, C. A.; Hein, B.; Jakobs, S.; Eggeling, C.; Hell, S. W. *Nat. Methods* **2008**, *5*, 943–945.
(17) Heilemann, M.; van de Linde, S.; Mukherjee, A.; Sauer, M. *Angew. Chem., Int. Ed.* **2009**, *48*, 6903–6908.
(18) Conley, N. R.; Biteen, J. S.; Moerner, W. E. *J. Phys. Chem. B* **2008**, *112*, 11878–11880.
(19) Wombacher, R.; Heidbreder, M.; van de Linde, S.; Sheetz, M. P.; Heilemann, M.; Cornish, V. W.; Sauer, M. *Nat. Meth.* **2010**, *7*, 717–721.
(20) Los, G. V.; et al. *ACS Chem. Biol.* **2008**, *3*, 373–382.
(21) O'Hare, H. M.; Johnsson, K.; Gautier, A. *Curr. Opin. Struct. Biol.* **2007**, *17*, 488–494.
(22) So, M.-K.; Yao, H.; Rao, J. *Biochem. Biophys. Res. Commun.* **2008**, *374*, 419–423.
(23) Lord, S. J.; Conley, N. R.; Lee, H. D.; Nishimura, S. Y.; Pomerantz, A. K.; Willets, K. A.; Lu, Z.; Wang, H.; Liu, N.; Samuel, R.; Weber, R.; Semyonov, A.; He, M.; Twieg, R. J.; Moerner, W. E. *ChemPhysChem* **2009**, *10* (1), 55–65.
(24) Schriven, E. F. V., Ed. *Azides and Nitrenes: Reactivity and Utility*; Academic Press: Orlando, FL, 1984.
(25) Shapiro, L.; McAdams, H. H.; Losick, R. *Science* **2009**, *326*, 1225–1228.
(26) Biteen, J.; Moerner, W. E. *Cold Spr. Harb. Persp. Biol.* **2010**, *2* (3), a000448.
(27) Bowman, G.; Comolli, L.; Gaietta, G.; Fero, M.; Hong, S.-H.; Jones, Y.; Lee, J.; Downing, K.; Ellisman, M.; McAdams, H.; Shapiro, L. *Mol. Micro.* **2010**, *76* (1), 173–189.
(28) McAdams, H.; Shapiro, L. *FEBS Lett.* **2009**, *583*, 3984–3991.
(29) Bernhardt, T. G.; de Boer, P. A. *Mol. Microbiol.* **2003**, *48*, 1171–1182.
(30) Dempsey, G.; Bates, M.; Kowtoniuk, W. E.; Liu, D. R.; Tsien, R. Y.; Zhuang, X. *J. Am. Chem. Soc.* **2009**, *131*, 18192–18193.

JA1044192